Journal of Achievements in Materials and Manufacturing Engineering
VOLUME 55
ISSUE 2
December
2012

# Alternate slicing and deposition strategies for fused deposition modelling of light curved parts

**B. Huang, S. Singamneni***
School of Engineering, AUT, Auckland, New Zealand
* Corresponding e-mail address: sarat.singamneni@aut.ac.nz

Received 14.10.2012; published in revised form 01.12.2012

**Analysis and modelling**

## ABSTRACT

Fused deposition modeling (FDM), as one of the additive manufacturing (AM) techniques, has been widely used in the manufacturing industry from the 1990s. It is relatively cheaper than other AM methods and there are other advantages such as being able to process a variety of other polymers. Currently, FDM is more likely to be suitable for direct production of the terminal-use parts, in some cases challenging traditional process such as injection molding. Research evidences indicate that change of road and layer structure would have significant influence on the meso-structure and thus impact the mechanical properties of the resulting polymer parts. Adaptive flat layer deposition and curved layer deposition have been introduced to improve the mechanical properties of terminal-use product. It is necessary that an appropriate deposition scheme is essential to ensure the best inter-road and inter-layer connectivity. Uninterrupted connections are likely to result in a continuous network of polymer chains, as in the case of the conventional processes. The current research proposes conventional flat layer deposition, adaptive flat layer deposition and curved layer deposition for FDM. In particular for curved parts, curved layer deposition in expected to ensure fiber continuity and better meso-structure. Mathematical models are developed for curved slicing, practically implemented to print physical parts and test results suggest marked improvement in the mechanical characteristics of curved parts.
**Keywords:** Fused deposition modeling; Additive manufacturing; Rapid prototyping

**Reference to this paper should be given in the following way:**
B. Huang, S. Singamneni, Alternate slicing and deposition strategies for fused deposition modelling of light curved parts, Journal of Achievements in Materials and Manufacturing Engineering 55/2 (2012) 511-517.

## 1. Introduction

Fused deposition modeling (FDM), as one of the additive manufacturing (AM) technologies, is applied to extrude the semi-molten plastic filament through a heated nozzle in a prescribed pattern onto the platform. The thermal energy associated with the semi-molten material drives the bonding, and it bonds with the surrounding material, cools and solidifies as the material is deposited [1]. Sintering process between roads and layers is completed by two consecutive steps. First, interfacial molecular contact is established by wetting, and then molecular moves towards preferred configurations to achieve the absorptive equilibrium. Molecules either diffuse or form chemical bonds across the interface and randomization can only be achieved through extensive inter-diffusion of chain segments under critical conditions, while the size of the neck growing indicates the quality of the bonding. However, the end result is that FDM parts partially bonded polymer filaments and voids, these defaults dominate the internal meso-structure of the FDM component.

Nowadays, FDM as a research topic has been widely study. Most of those studies are concentrated in three main categories: deposition materials, internal meso-structure, and external accuracy. In terms of deposition material, most of the researches are focus on the non thermal plastics and thermal plastics expect Acrylonitrile-Butadiene-Styrene (ABS). For the non thermal plastics and composite, Danforth et al [2] introduced technique in to fused deposition of ceramics and Jafari [3] et al further extended it to fused deposition of multiple ceramics (FDMC) by using multi-material ceramics. Polymer composites, like Metal/polymer materials [4], also has been developed by consisting of iron particles in a nylon type matrix, as well as the piezocomposite [5]. For thermal plastics, different polymers, as well as the polymer composites have been tried. Medical-grade polymethylmethacrylate (PMMA) [6], polypropylene [7], and polycaprolactone [8] were tried with FDM technique.

The mechanical property is also one of the main factors to evaluate the FDM component. The major controlling factor for the mechanical properties of FDM parts is the meso-structure. Rodriguez et al [9] investigated with unidirectional P400 ABS plastic material parts built with FDM 1600 machine. They quantified the nature and range of the meso-structural tailoring capability of the FDM materials. Then, they clearly elucidated the need for further research aimed at process improvements. Further experimental evaluation of the influence of the meso-structure on mechanical properties showed significant meso-structural influence on the stress-strain response [10]. It is noted that elastic and shear moduli values 11-37 per cent lower and yield strength values 22-57 per cent lower than the ABS monofilament. The same will also fall short of the injection molded counterparts. Adhesive strength between layers or across filaments is weaker than the strength of continuous filaments [11] and the air gap and raster orientation affect the tensile strength of FDM parts dramatically. While layer thickness, road width and speed by far remain the most significant parameters influencing the form and surface quality of prototypes [12], in some specific cases, for example, the thin shell components, discontinuous filament structure deteriorates the part strength even further.. Also, the build style and road structure would have significant influences on the final part characteristics. Build direction effective from either the orientation of the deposition head [13] or the part orientation itself [14] could have significant influences on the part properties and build times.

Apart from material and internal mechanical property external accuracy also affects the FDM components. The external surfaces are affected by stair-step effects resulting from the stacking of flat layers and the part orientation, especially by using thicker layers. In order to build the part more accurately, the number of layers needs to be increased, by reducing the thickness of the flat layers [15] often leading to unacceptable build times. Slicing algorithms also significantly influence the part quality and build times and the following are some prominent attempts in this direction; Jamieson and Hacker [16] attempted direct slicing of CAD models and observed enhanced dimensional accuracy and reduced processing times. While Kulkarni and Dutta [17] implemented adaptive slicing based on variable thickness slicing for optimum number of slices and cusp-height, Sabourin et al. [15] used stepwise uniform refinement, resulting in reduced build time, without losing the overall accuracy. Hope et al. [18] developed an adaptive slicing procedure based on surface curvature and angle of the surface normal for the best geometric accuracy. Luo et al. [19] proposed an efficient 3D slicing considering both the part and support structures. Yang et al. [20] showed significant improvements in both process efficiency and part quality through equidistant path generation from both experimental and simulation analyses.

General improvements of the FDM component were made based on those studies. However, for some particular case, further shortcomings are rising. The hypothesis for this research is that in the case of curved parts such as the one shown in Fig. 1a, curved layer slicing and deposition as shown in Fig. 1c result in better material structure and consequent part strength, due to fiber continuity, as against the conventional flat layer deposition as shown in Fig. 1b. One of the immediate solutions is to slicing this particular part with curved layer then processing following the curved slicing.

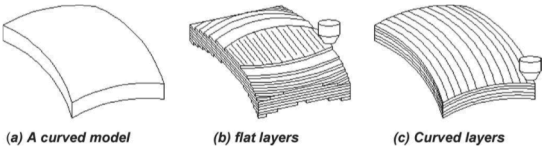


Fig. 1. Curved layer fused deposition modelling (CLFDM) (a) curved model (b) Flat layers slicing strategy (c) Curved layers slicing strategy

Klosterman et al. [21] developed a curved layer process based on laminated object manufacturing (LOM) technology for efficient production of curved layer parts. Monolithic ceramic (SiC) and CMC (SiC/SiC) articles were fabricated using Curved Layer Laminated Object Manufacturing (CLLOM). For making curved objects, the CLLOM process allowed advantages of eliminated stair step effect, increased building speed, reduced waste, and maintenance of continuous fibers in the direction of curvature.

Chakraborty et al. [22] developed a curved layer fused deposition modeling (CLFDM) algorithm which was formulated and tested on parametric surfaces. The mathematical models they built up were theoretical. It is evident that adaptive slicing is attempted by different means, but most of these approaches remained as mathematical models only and not until recently, Singamneni et al practically implemented the CLFDM in reality [23], as well as the basic adaptive FDM. The current research starts from here and attempt to compare the FDM deposition strategies for a given curved part and aim to find out the best deposition strategies for the general curved FDM components. The test spices were built by conventional flat layer FDM, adaptive flat layer FDM and CLFDM. All the spices are subsequent tested by three-point bending test and the result are evaluated. The result will be used to determine the proper deposition strategy for the particular part.

## 2. Generation of slice data

The STL file is the de facto standard file format for AM currently and gathering the facet data from STL files is the

compulsory process for all the slicing strategies. A STL file model, as shown in Fig. 2 can be created by any 3D engineering solid modeling software. As these files are in the binary form, it is hard to gather the facet data and an open source MATLAB program was created to process this work. The STL format file is used to process slicing data of test parts considered in this paper.

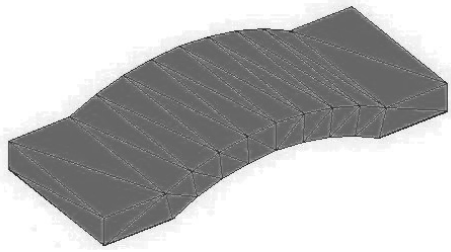

Fig. 2. Standard STL file

## 2.1. Conventional slicing strategy

To gather the data from Binary STL format file, it normally follows the procedure as show as follows in Figure 3.

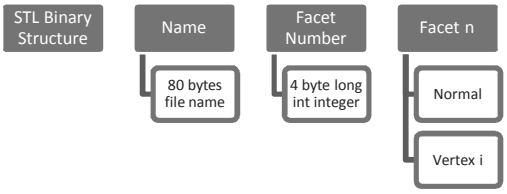


Fig. 3. Procedure of gathering data from Binary STL format

1. Get 80 bytes information from STL file for the file name.
2. Get 4 bytes for the total number of the facets in the STL file.
3. Get three 32-bit-floating point numbers from individual facet data for the normal.
4. Get the rest 32-bit-floating point numbers for X, Y and Z coordinates of each vertex.

All the vertexes in every facet are following the counter clockwise direction, which follows the right hand law, as well as the normal of the facet, to indicate the external and internal part of the STL file, as shown in Figure 4.

All the data is gathered from the Binary STL file, and then they are sort in matrix form, as shown in Figure 5, for the further slicing calculation.

After all the information of the STL file is collected, the slicing algorithm can be implemented. Slicing a STL file through intersecting the model with the XY plane at each Z increment is a well-known method of slicing method.

A series of offset horizontal planes are used to slicing the STL. The intersection line from horizontal planes and facets on the STL file will be gathered. For getting the intersection lines from the STL file, the most common way to do that is cutting the edge of the triangular facets as shown in Figure 6.

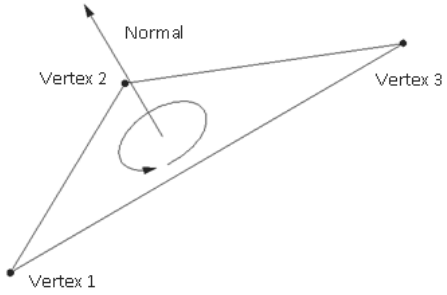


Fig. 4. Data information of every single facet

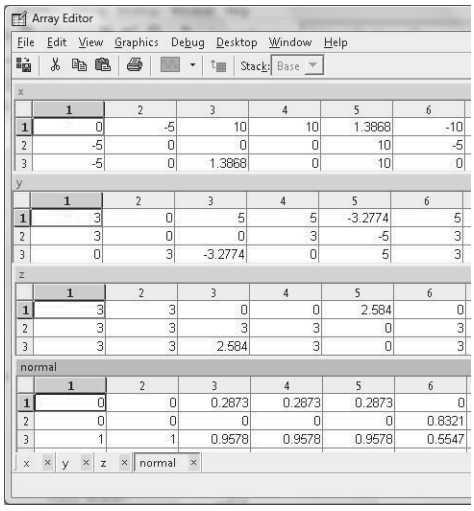


Fig. 5. Data information of binary STL file

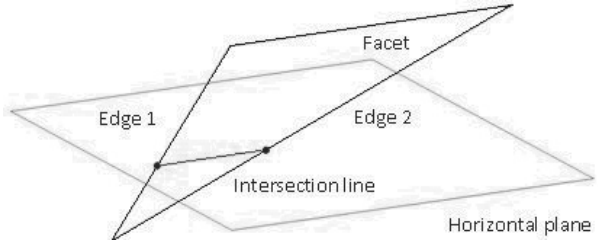


Fig. 6. Facet slicing based on line intersection

The mathematical expression for the slicing algorithm is shown in Equation (1).

$$x = x_1 + \frac{z_1 - z_{sliced}}{z_1 - z_2} \cdot (x_2 - x_1) \quad (1)$$

$$y = y_1 + \frac{z_1 - z_{sliced}}{z_1 - z_2} \cdot (y_2 - y_1) \quad (2)$$

where

$$z_1 \le z_{sliced} \le z_2 \,;\; z = z_{sliced}$$

Or there is an alternate mathematical expression, which constructs an additional plane as shown in Figure 7.

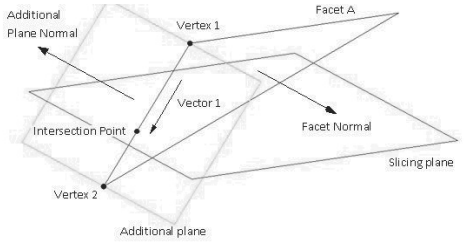


Fig. 7. Facet slicing based on plane intersection

The mathematical expression of a random flat plane is $ax + by + cz + d = 0$, and the normal of the plane is (a, b, c).

Assume that Facet A is $a_1x + b_1y + c_1z + d_1 = 0$ and Slicing plane is $a_2x + b_2y + c_2z + d_2 = 0$.

Slicing plane could be any angle, not necessary to be horizontal.

To get the mathematical expression of additional plane, it follows this method:

1. Normal, and
2. A point on the plane.

As we known, vector 1, which can be obtained by vertex 1 and 2, is one of the vector lie on additional plane. For simplifying the calculation, assume the additional plane is totally perpendicular to Facet A, Facet Normal is another vector can be obtained. Then cross product vector 1 and Facet Normal, the Additional Plane Normal can be calculated, say $(a_3, b_3, c_3)$.

And then, substitute the Additional Plane Normal into mathematical expression of a random flat plane. Owing to either Vertex 1 or 2 is a point on the additional plane, assume Vertex 1 is substitute x, y and z in the mathematical expression, $d_3$ can be calculated.

So the mathematical expression of additional plane is $a_3x + b_3y + c_3z + d_3 = 0$.

Put the expressions in the matrix form:

$$\begin{pmatrix} a_1 & b_1 & c_1 \\ a_2 & b_2 & c_2 \\ a_3 & b_3 & c_3 \end{pmatrix} \begin{pmatrix} x \\ y \\ z \end{pmatrix} = \begin{pmatrix} -d_1 \\ -d_2 \\ -d_3 \end{pmatrix} \tag{3}$$

The intersecting point can be calculated afterwards. Repeat the same processing for all the intersecting facets, the coordinates of all intersecting points is gathered. The slicing profile of the STL file in conventional slicing is shown in Figure 8.

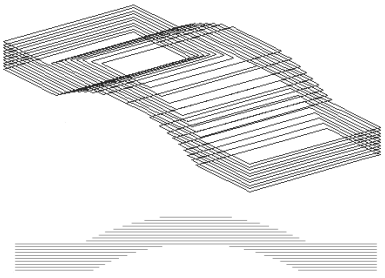

Fig. 8. Conventional slicing contour of STL file

## 2.2. Adaptive slicing strategy

For the uniform flat layer slicing, the slicing plane only needs to increase a fixed distance on every layer. However, for adaptive flat layer slicing, the thickness of each layer might not be the same. In order to select the proper thickness for slicing, cusp height concept is introduced in the processing.

The cusp height (h), as shown in Figure 9, is a commonly used measure of the well documented stair step effect. The largest angle over all facets in the slicing plane is denoted as β. A user specified cusp height is h. the maximum allowable layer thickness ($t_{max}$) which satisfied the cusp height constraint for a given slice plane is:

$$t_{max} = \frac{h}{\sin\beta} \tag{4}$$

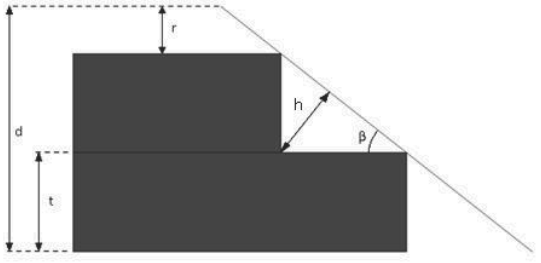


Fig. 9. Definition of cusp height (h)

From the previous researches, people tried to use cusp height (h) and largest angle (β) to define the maximum thickness of the layer. However, in this application, the thickness option is defined and the cusp height is assumed to be 0.2 mm. Then, the largest angle is only unknown in Equation 4.

Owing to two types of different thickness are available, then equation 3 can be rewritten as shown below:

$$\beta = \operatorname{asin}\left(\frac{h}{t}\right) \tag{5}$$

Based on Equation 3 and the preset cusp height (h), four types of different thickness layer can be categorized into four angle range as shown in the Table 1.

Table 1.
Relationship between layer thicknesses and angle range

| Layer thickness | Angle |
|---|---|
| 0.4 mm | [0, 15°] |
| 0.8 mm | [15°, 90°] |

Apart from the angle domains, the shape of the facet involved is also a factor affecting the adaptive slicing. For the general STL file, a situation exists like this: the facet is greater than 15° but the shape is less than the maximum layer thickness. Further, if the facet has been slicing and only small area need to be sliced, this situation would similar to the small facet. In this case, the rest height concept is also introduced for the adaptive slicing and a further slicing criterion is used as shown in Table 2.

Table 2.
Relationship between layer thicknesses and rest height

| Layer thickness | Rest Height |
|---|---|
| 0.4 mm | $\Delta h < 1.0$ |
| 0.8 mm | $\Delta h > 1.0$ |

Once the STL file is sliced, the angle between each sliced facet and the slicing plane is calculated and store into a matrix. The angle values might be different, so the minimum angle value determinates of the angles. After all the layer thicknesses are properly set, the slicing process is started gather the data from Binary STL format file, similar to the conventional slicing process. The adaptive slicing contour of STL file as shown in Fig. 10.

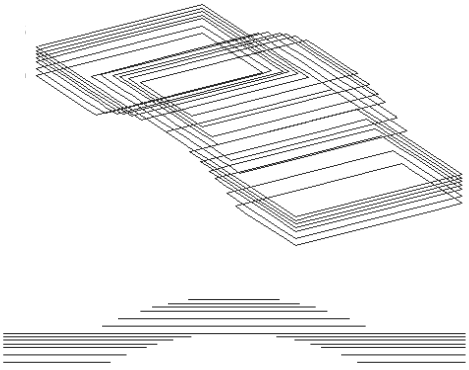

Fig. 10. Adaptive slicing contour of STL file

## 2.3. Curved layer slicing strategy

Similar to flat layer slicing, the data will be gathering from STL format file. This mechanism of offsetting is to offset every triangular facet individually in a certain distance, and then reconstruct those offset facets back together.

First of all, the facets on the top surface area are grouped together. After the grouping, facets would be offset a layer down following their sequence. Every single facet would be considered as a spatial plane and its mathematical equation is:

$$ax + by + cz + d = 0 \tag{6}$$

Where, a, b and c is x y and z directions of normal vector, d is the offset distance of the facet.

The offset distance is thickness of the deposition filament (t). After offsetting, the equation of offset facet is:

$$ax + by + cz + (d + t) = 0 \tag{7}$$

All the top facets are offset following this basic offsetting processing. However, this new facet is only a spatial plane without the boundary. If their boundaries are not found, all the offsetting facets will intersect to each other and the non-offsetting facets. In order to get the new boundary for the offset plane, the relationships between planes before the offsetting need to be recorded down. Owing to the complexities of the basic object is not high; the relationships are maintained after offsetting. Every vertex on the facet is linking to at least other facets, and there would be the boundary of the new offsetting facet, as shown in Fig. 11.

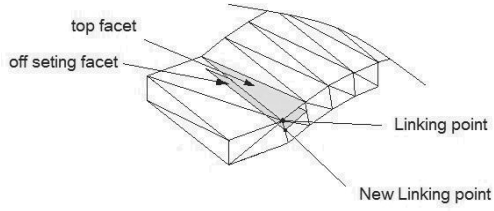


Fig. 11. Boundary of top facet and offsetting facet

Owing to the vertex on the original facet link to at least two adjacent facets, If the offset distance is not exceed the area of adjacent facets, three planes algorithm can be used here. The equation of original facet is:

$$a_1x + b_1y + c_1z + d_1 = 0 \tag{8}$$

And the equations of adjacent facets are:

$$a_2x + b_2y + c_2z + d_2 = 0 \tag{9}$$
$$a_3x + b_3y + c_3z + d_3 = 0 \tag{10}$$

If the offset distance equals to the thickness of the layer, then the equation of new offset is:

$$a_1x + b_1y + c_1z + (d_1 + t) = 0 \tag{11}$$

Put the expressions in the matrix form:

$$\begin{pmatrix} a_1 & b_1 & c_1 \\ a_2 & b_2 & c_2 \\ a_3 & b_3 & c_3 \end{pmatrix} \begin{pmatrix} x \\ y \\ z \end{pmatrix} = \begin{pmatrix} -d_1 - t \\ -d_2 \\ -d_3 \end{pmatrix} \tag{12}$$

The new vertex on the offsetting facet can be calculated afterwards. Repeat the same way, other two vertices of the offsetting facet also can be done.

Repeat this algorithm, all the facets in the facet group are offset and the first offset curved layer is generated as shown in Fig. 12 below.

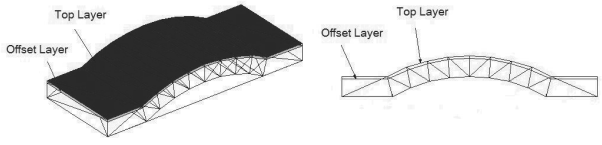


Fig. 12. Offset layer

After the first offset layer was done, first offset layer would replace the top layer and become the referencing layer. The second offset layer would be generated based on the first offset layer. This replacing procedure would be continued until the last offset layer finish. The entire procedure is shown in Fig. 13.

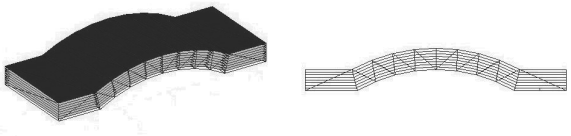

Fig. 13. Basic curved layer offsetting

## 3. Practical implementation for all the deposition strategies

Commercial FDM machines usually work as black boxes, and do not allow much freedom to alter process conditions. Make-shift test facilities could be built, but will have limitations on the quality of controlling the parameters. Several case studies for different slicing process are then considered for the testing and a test bed is assembled procuring a Makerbot system for the practical implementation of the models. A geometrical shape with typical features including a curved surface is considered for this purpose with the general size 50 X 20 X 10, the STL model of which is as shown above in Fig. 2.

The main limitation is the test platform. The feed mechanism between xy axis and z axis are different, one is using pulleys and bell, which speed can up to 4000 mm/min, while the other using the thread rod that only has the 120 mm/min max speed. This huge speed difference the material not able to deposition for the part with big curvature feature, especially for CLFDM. Another difficulty is the extrusion control, which is not able to provide enough torque and speed range. This will affect the flow of material through the extruded nozzle. A more practical test platform is now in the upgrading and once this setup is ready, the big curvature feature parts will be tested. In order to overcome these difficulties, a proper MATLAB program is made to handle the practical situation by maximizing the limits of the DC motor. Tool path and parameter settings also generated by the same program as shown in Fig. 14.

## 4. Testing

The test piece produced using natural ABS filament as the fused material is shown in Fig. 15. The next step is to use all the specimens from different deposition strategies for a comparative analysis of mechanical performance.

A three point bending test conducted and revealed different loads from those specimens as shown in Table 3.

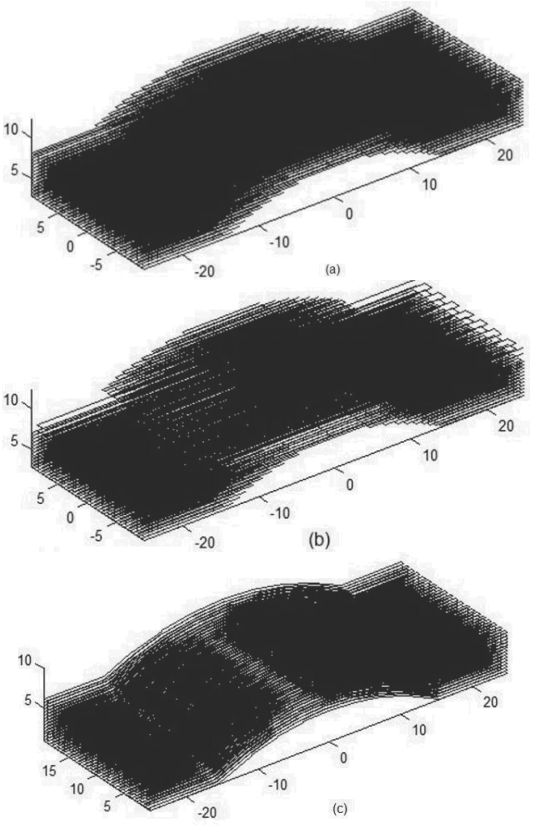


Fig. 14. Tool paths for deposition strategies (a) conventional flat layer deposition (b) Adaptive flat layer deposition (c) Curved layer deposition

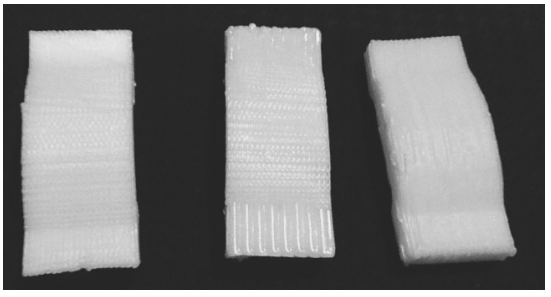

Fig. 15. Test piece produced using natural ABS filament as the fused material

Table 3.
Result from three point bending test

| Deposition strategies | Maximum compressive load (N) | | | | Average (N) | Standard deviation |
|---|---|---|---|---|---|---|
| | Part 1 | Part 2 | Part 3 | Part 4 | | |
| Conventional Flat layer slicing | 582.666 | 582.333 | 691.666 | 649.333 | 626.500 | 46.476 |
| Adaptive Flat layer slicing | 806.000 | 702.333 | 863.000 | 687.333 | 764.666 | 72.876 |
| Curved layer slicing | 963.000 | 926.333 | 986.000 | 930.333 | 951.417 | 24.515 |

## 5. Results and analysis

The experimental data in terms of the maximum compress load in each case is compiled in Table 2 for a statistical evaluation of the comparative performance of all the different deposition strategies FDM. The average compressive load in the case of conventional flat layered components falls short by almost 140 N compared to the adaptive layer parts, while the adaptive layer parts have almost close to 200 N less than the curved layer counterpart. It clearly indicates a huge difference mechanical performance among those three deposition strategies and CLFM has the best mechanical performance in the three point bending test.

## 6. Conclusions

Algorithms for all different deposition strategies are reviewed, and the curved layer slicing algorithm is improved. All the FDM components are successfully and physically implemented by the same machine. Experimental results indicate the curved layer deposition strategy has the best mechanical property in terms of curved part, followed by the adaptive layer deposition and the conventional flat layer. The average fracture compressive load of curved parts less than three point bending increased almost 28% and 42% compared to that of the adaptive layer and conventional flat layer counter parts. This could be attributed to use different deposition strategies into different situation to improve the meso-structure.

## Acknowledgements

We extend our sincere thanks to all the technicians for their help. We also thank School of Engineering, AUT providing all the experimental equipment.

## References

[1] C.T. Bellehumeur, L. Li, Q. Sun, P. Gu, Modelling of bond formation between polymer filaments in the fused deposition modelling process, Journal of Manufacturing Processes 6 (2004) 170-178.

[2] S.C. Danforth, A. Safari, Solid free form fabrication, novel manufacturing opportunities for electroceramics, Proceedings of the 10th IEEE International Symposium 1 (1996) 183-188.

[3] M.A. Jafari, W. Han, F. Mohammadi, A. Safari, S.C. Danforth, N. Langrana, A novel system for fused deposition of advanced multiple ceramics, Rapid Prototyping Journal 6 (2000) 161-175.

[4] S.H. Masood, W.Q. Song, Development of new metal/polymer materials for rapid tooling using Fused deposition modelling, Materials and Design 25 (2004) 587-594.

[5] A. Bandyopadhyay, K. Raj. Panda, F. Victor. Janas, K. Mukesh. Agarwala, C. Stephen, S.C. Danforth, A. Safari, Processing of piezocomposites by fused deposition technique, Journal of the American Ceramic Society 80 (1997) 1366-1372.

[6] D. Espalin, K. Arcaute, D. Rodriguez, F. Medina, M. Posner, R. Wicker, Fused deposition modeling of patient-specific polymethylmethacrylate implants, Rapid Prototyping Journal 16 (2010) 164-173.

[7] P. Ng, P.S.V. Lee, J.C.H. Goh, Prosthetic sockets fabrication using rapid prototyping technology, Rapid Prototyping Journal 8 (2002) 53-59.

[8] D.W. Hutmacher, T. Schantz, I. Zein, K.W. Ng, S.H. Teoh, K.C. Tan, Mechanical properties and cell cultural response of polycaprolactone scaffolds designed and fabricated via fused deposition modeling, Journal of Biomedical Materials Research 55 (2001) 203-216.

[9] J.F. Rodríguez, J.P. Thomas, J.E. Renaud, Characterisation of the mesostructure of fused deposition acrylonitrile butadiene-styrene materials, Rapid Prototyping Journal, Rapid Prototyping Journal 6 (2000) 176-185.

[10] J.F. Rodríguez, J.P. Thomas, J.E. Renaud, Mechanical behaviour of acrylonitrile butadiene styrene (ABS) fused deposition materials, experimental investigation, Rapid Prototyping Journal 7 (2001) 148-158.

[11] C.S. Lee, S.G. Kim, H.J. Kim, S.H. Ahn, Measurement of anisotropic compressive strength of rapid prototyping parts, Journal of Material Processing Technology 187-188 (2007) 627-630.

[12] R. Anitha, S. Arunachalam, P. Radhakrishnan, Critical parameters influencing the quality of prototypes in fused deposition modelling, Journal of Material Processing Technology 118 (2001) 385-388.

[13] F. Xu, H.T. Loh, Y.S. Wong, Considerations and selection of optimal orientation for different rapid prototyping system, Rapid Prototyping Journal 5 (1999) 54-60.

[14] Z. Hu, K. Lee, J. Hur, Determination of optimal build orientation for hybrid rapid-prototyping, Journal of Material Processing Technology 130-131 (2002) 378-383.

[15] E. Sabourin, S.A. Houser, J.H. Bohn, Adaptive slicing using stepwise uniform refinement, Rapid Prototyping Journal 2 (1996) 20-26.

[16] R. Jamieson H. Hacker, Direct slicing of CAD models for rapid prototyping, Journal of Rapid Prototyping 1/2 (1995) 4-12.

[17] P. Kulkarni, D. Dutta, An accurate slicing procedure for layered manufacturing, Computer Aided Design 28 (1996) 683-697.

[18] R.L. Hope, R.N. Roth, P.A. Jacobs, Adaptive slicing with sloping layer surfaces, Rapid Prototyping Journal 3 (1997) 89-98.

[19] R.C. Luo, P.T. Yu, Y.F. Lin, H.T. Leong, Efficient 3D CAD model slicing for rapid prototyping manufacturing system, Proceeding of Industrial Electronics Society IEEE 3 (1999).

[20] Y. Yang, J.Y. H. Fuh, H.T. Loh, Y.G. Wang, Equidistanct path generation for improving scanning effciency in layered manufacturing, Rapid Prototyping Journal 8 (2002) 30-37.

[21] D.A. Klosterman, R.P. Chartoff, N.R. Osborne, G.A. Graves, A. Lightman, G. Han, A. Bezeredi, S. Rodrigues, Development of a curved layer LOM process for monolithic ceramics and ceramic matrix composites, Rapid Prototyping Journal 5 (1999) 61-71.